Networked ISAC Coordinated Beamforming and Cooperative BS Cluster Optimization

Kaitao Meng
University College London, London, UK
kaitao.meng@ucl.ac.uk

Christos Masouros
University College London, London, UK
c.masouros@ucl.ac.uk

***Abstract*—In this work, we study integrated sensing and communication (ISAC) networks to optimize and balance the sensing and communication (S&C) performance. Using stochastic geometry, we analyze S&C performance by deriving tractable expressions for area spectral efficiency (ASE), based on which, we optimize cooperative base station cluster sizes for S&C, along with user/target numbers, to achieve a flexible S&C tradeoff. It is shown that interference cancellation significantly improves the average data rate and the radar information rate. Interestingly, optimal communication tradeoffs aimed at maximizing ASE mainly emphasize spatial resource utilization for multiplexing and diversity gain without interference nulling. Conversely, for sensing objectives, resource allocation tends towards interference cancellation. Simulation results confirm that our proposed cooperative ISAC scheme significantly improves S&C performance.**

I. Introduction

Integrated sensing and communication (ISAC), as a candidate for sixth generation (6G) communications, can provide both sensing and communication (S&C) services with a unified infrastructure/waveform/network, thereby overcoming the problems of spectrum scarcity and severe interference [1], [2]. ISAC offers an exciting opportunity not only to improve spectrum efficiency, but also to enable hardware reuse, power savings and the development of various environment-aware applications envisioned for 6G systems [3]. In the literature, most existing works on this topic mainly focus on the system design and optimization in single cell [4], while multi-cell ISAC is seldom investigated.

In large-scale dense ISAC networks, inter-cell interference emerges as a critical constraint limiting network performance. Coordinated beamforming presents a promising solution to mitigate inter-cell interference, thus significantly enhancing the S&C performance of the whole network [5]. Furthermore, network-level ISAC introduces new performance metrics, novel coordination frameworks, and extra degrees of freedom (DoF) for balancing S&C performance. For instance, it allows for the control of cooperative base station (BS) cluster sizes and the average numbers of served users/targets to enhance S&C performance. However, quantitatively analyzing average network performance for S&C in ISAC networks is highly non-trivial, especially when considering the effects of random channel fading and spatial locations.

In the literature, stochastic geometry becomes a powerful mathematical tool for the analysis of multi-cell wireless communication networks [6], [7]. For instance, the authors in [6] proposed a general framework for analysis of the average data rate and the coverage probability in communication networks. Besides evaluating the performance of communication-only networks or sensing-only networks, stochastic geometry may also be adopted for the performance analysis of ISAC networks. For example, in [8], an ISAC beam alignment approach for THz networks was investigated, where stochastic geometry was employed to derive expressions for coverage probability and network throughput. In [9], closed-form expressions for energy efficiency (EE) in ISAC networks were derived to maximize the network EE by optimizing the BS density. However, the aforementioned works focus solely on serving one user/target per cell and o not take into account inter-cell interference management. Thus, this approach fails to fully exploit the multiplexing gain inherent in spatial resources.

Motivated by the above discussion, our study investigates a cooperative ISAC scheme aimed at optimizing S&C performance at the network level. Leveraging stochastic geometry tools, we conduct a comprehensive performance analysis, elucidating critical cooperative dependencies within the ISAC network. Then, we derive the tractable S&C area spectral efficiency (ASE) expression to analyze three kinds of system objectives of spatial resource allocation, including serving multiple users/targets for *spatial multiplexing gain*, *spatial diversity gain*, and *inter-cell interference nulling*. This analysis provides valuable insights to facilitate a closer inspection of specific features and emerging trends. Furthermore, we prove that it is not necessary to perform interference nulling when maximizing the communication ASE under some general parameter setups; in contrast, interference nulling is required when maximizing the sensing ASE.

II. System Model

In this study, we introduce a coordinated beamforming approach aimed at achieving adaptable interference nulling within ISAC networks. Our method involves each BS transmitting independent data to K users, while concurrently conducting sensing operations for J targets (e.g., localization) by using unified ISAC signals. To suppress S&C interference separately, Q (L) closest BSs are selected for interference nulling of sensing (communication). By forming separate S&C cooperative clusters according to the locations of targets and users, the corresponding beamforming vectors of Q BSs (L BSs) are jointly designed for interference nulling of sensing

(communication), as depicted in Fig. 1. In the considered system, M_{t} (M_{r}) transmit (received) antennas are deployed at each BS, whose location follows a homogeneous Poisson point process (PPP), denoted by $\Phi_b = \{\mathbf{d}_i \in \mathbb{R}^2\}$, where $\mathbf{d}_i$ represents the location of BS i. Similarly, the point processes of the locations of single-antenna communication users and targets are respectively denoted by Φ_u and Φ_t. Here, Φ_b, Φ_u, and Φ_t are assumed to be mutually independent PPPs with intensities λ_b, λ_u, and λ_s, where $\lambda_u, \lambda_s \gg \lambda_b$ [7].

The typical user, identified as user k, is assumed to be positioned at the origin, and its performance is analyzed for representing the average performance for all users [7]. The typical user is served by its nearest BS (referred to as the serving BS), identified by index 1. Then, the received signal at the typical user k can be expressed as

$$y_{c,k} = \|\mathbf{d}_1\|^{-\frac{\alpha}{2}} \mathbf{h}_{k,1}^H \mathbf{W}_1 \mathbf{s}_1 + \sum_{i=2}^{\infty} \|\mathbf{d}_i\|^{-\frac{\alpha}{2}} \mathbf{h}_{k,i}^H \mathbf{W}_i \mathbf{s}_i + n_{k,c}, \tag{1}$$

where $\alpha \geq 2$ is the pathloss exponent, $\mathbf{h}_{k,i}^H \sim \mathcal{CN}(0, \mathbf{I}_{M_{\mathrm{t}}})$ is the channel vector from BS at $\mathbf{d}_i$ to user k, $\mathbf{W}_i = \left[\mathbf{w}_1^i, \ldots, \mathbf{w}_K^i\right] \in C^{M_{\mathrm{t}} \times K}$ is the beamforming matrix of the BS at $\mathbf{d}_i$, and $\mathbf{s}_i = \left[s_1^i, \ldots, s_K^i\right]^T$ is the information symbol vector transmitted from the corresponding BS with equal power allocation.

In response to severe interference in dense cell scenarios, this work concentrates on an interference-limited network where noise can be disregarded, employing the signal-to-interference ratio (SIR) as the basis for performance evaluation [10]. The BS located at $\mathbf{d}_i$ employs zero-forcing beamforming $\mathbf{W}_i$, distributing equal power among the K users, thereby suppressing intra-cluster S&C interference and optimizing the desired signal strength for all K users within the cluster. Then, the SIR at the typical user can be given by

$$\mathrm{SIR}_c = \frac{g_{k,1}^k \|\mathbf{d}_1\|^{-\alpha}}{\sum_{i=L+1}^{\infty} g_{k,i} \|\mathbf{d}_i\|^{-\alpha}}, \tag{2}$$

where $g_{k,1}^k = \left|\mathbf{h}_{k,1}^H \mathbf{w}_k^1\right|^2$ and $g_{k,i} = \sum_{j=1}^{K} \left|\mathbf{h}_{k,i}^H \mathbf{w}_j^i\right|^2$. In this work, we adopt ASE [11] as the network-level communication performance metric. Then, the mathematical expression for the communication ASE is given by

$$T_c^{\mathrm{ASE}} = \lambda_b K R_c, \tag{3}$$

where $R_c = \mathrm{E}[\log(1 + \mathrm{SIR}_c)]$ denotes the average data rate.

Likewise, the typical target, denoted as target j, is positioned at the origin and sensed by the nearest BS situated at $\mathbf{d}_1$. The large-scale pathloss fading from the target to the serving BS is modeled as $|\mathbf{d}_1|^{-2\beta}$, where $\beta \geq 2$ represents the pathloss exponent from the serving BS to the typical target. Each BS designs its respective receive filter directed towards the direction of target j's direction θ_j. To maintain tractability in our analysis, we adopt the maximum-ratio combining receive filter $\mathbf{v}j^H(\theta_j) = [1, \cdots, e^{-j\pi(M\mathrm{r}-1)\cos(\theta_j)}]^T$, since it strikes a balance between performance and analytical convenience.

After the operation of receive filtering for target j, the corresponding received signal at the serving BS is given by

$$y_{s,j} = \mathbf{v}_j^H(\theta_j) \|\mathbf{d}_1\|^{-\beta} \mathbf{b}(\theta_j) \mathbf{a}^H(\theta_j) \mathbf{W}_1 \mathbf{s}_1 (t - 2\tau_{j,1}) + \sum_{q=2}^{\infty} \|\mathbf{d}_q - \mathbf{d}_1\|^{-\frac{\alpha}{2}} \mathbf{h}_{q,1}^H(\theta_j) \mathbf{W}_q \mathbf{s}_q (t - \tau_{q,1}) + \mathbf{v}_j^H \mathbf{n}_s, \tag{4}$$

where $\mathbf{a}^H(\theta_j) = [1, \cdots, e^{j\pi(M_{\mathrm{t}}-1)\cos(\theta_j)}]^T$, $\mathbf{b}(\theta_j) = [1, \cdots, e^{j\pi(M_{\mathrm{r}}-1)\cos(\theta_j)}]$, $\mathbf{h}_{q,1}^H(\theta_j) = \mathbf{v}_j^H(\theta_j) \mathbf{G}_{q,1}^H$, and $\|\mathbf{d}_q - \mathbf{d}_1\|$ represents the distance from the interfering BSs at $\mathbf{d}_q$ to the serving BS. In (4), $\tau_{j,1}$ and $\tau_{q,1}$ respectively represent the transmission delay of target-serving BS link and BS q-serving BS link. The transmit beamforming of BS q in the cooperative cluster is designed based on the interference channel from BS q to the serving BS and the receive filter. Then, with a matching filter over the symbol domain, the SIR of echo signals reflected from the typical target can be given by

$$\mathrm{SIR}_s = \xi \Delta T \kappa M_{\mathrm{r}} \frac{h_{j,1}^t \|\mathbf{d}_1\|^{-2\beta}}{\sum_{q=Q+1}^{\infty} h_{q,1} \|\mathbf{d}_q - \mathbf{d}_1\|^{-\alpha}}, \tag{5}$$

where $h_{j,1}^t = \sum_{k=1}^{K} \left|\mathbf{a}^H(\theta_j) \mathbf{w}_k^1\right|^2$ is the effective signal channel gain from the serving BS towards the target's direction, $\sum_{q=Q+1}^{\infty} h_{q,1} \|\mathbf{d}_q - \mathbf{d}_1\|^{-\alpha}$ is the inter-cluster interference, and $h_{q,1} = \sum_{k=1}^{K} \left|\mathbf{h}_{q,1}^H(\theta_j) \mathbf{w}_k^q\right|^2$. In equation (5), ΔT represents the matching filter gain, $\kappa \in [0, 1]$ denotes the mismatch loss of the receiving filter, and ξ signifies the radar cross-section (RCS) of the target. Typically, the maximum distinguishable number of targets, $J_{\max}$, is constrained by factors such as the number of receive antennas and processing time requirements.

In previous studies, it has been observed that higher information rates between the target impulse response and measurements lead to improved radar capabilities [12]. Consequently, radar information rate serves as a suitable metric for assessing the accuracy of system parameter estimation. Then, we introduce the concept of sensing ASE to comprehensively characterize the network-level performance of ISAC. The mathematical expression for sensing ASE is

$$T_s^{\mathrm{ASE}} = \lambda_b J R_s, \tag{6}$$

where $R_s = \mathrm{E}[\log(1 + \mathrm{SIR}_s)]$ is the target' average radar information rate.

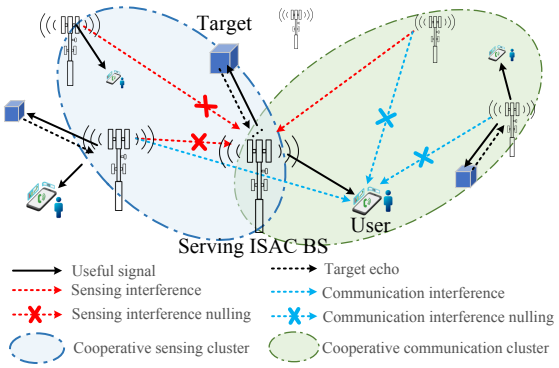

Fig. 1. Cooperative ISAC networks with S&C interference nulling.

III. Sensing and Communication Performance

A. Communication Performance

According to [13], under a given distance r from the typical user to the serving BS, the conditional expectation can be derived as follows:

$$\mathrm{E}\left[\log\left(1+\mathrm{SIR}_c\right)|r\right]=\mathrm{E}\left[\log\left(1+\frac{g_{k,1}^{k}}{\sum_{i=L+1}^{\infty} g_{k,i}\|\mathbf{d}_i\|^{-\alpha} r^{\alpha}}\right)\right]. \tag{7}$$

In the following, we exploit the mean interference-to-signal-ratio (MISR)-based gain method [14] to analyze the average rate and obtain a more tractable expression in Theorem 1.

Theorem 1: The communication rate can be approximated as

$$T_c^{\mathrm{ASE}}=\lambda_b K\int_0^{\infty}\frac{1-e^{-zY(K,L,J,Q)}}{z\mathrm{F}(z,\alpha)}dz, \tag{8}$$

where $\mathrm{F}\left(z,\alpha\right) = \left(e^{-z}-1\right)+z^{\frac{2}{\alpha}}\Gamma\left(1-\frac{2}{\alpha},z\right)$ and $Y(K,L,J,Q)=\frac{\Gamma\left(L+\frac{\alpha}{2}\right)(M_{\mathrm{t}}-J(Q-1)+1-KL)}{K\Gamma(L+1)\Gamma\left(1+\frac{\alpha}{2}\right)}$.

Proof: Please refer to Appendix A. ■

Theorem 1 provides a more tractable form of the the communication ASE. It is verified that (8) achieves a good approximation by Monte Carlo simulations, as shown in Section V. It can be observed that only the term $Y(K,L,J,Q)$ in (8) involves cooperative cluster sizes L and Q. In addition, the optimal L^* must belong to the range $[1,\frac{M_{\mathrm{t}}-J(Q-1)+1}{K}-1]$. Thus, with any given K, the optimal cluster size can be obtained by calculating $\frac{\partial Y(K,L,J,Q)}{\partial L}=0$. However, it is still difficult to analyze the optimal cooperative cluster size, since the specific relationship of the Gamma function on L is unclear if α takes any value. To draw useful insights, we prove the optimal number of cooperative clusters under some typical parameters in wireless cellular networks.

Proposition 1: When $\alpha=4$, the optimal $L^*=1$ when T_c^{ASE} is maximized.

Proof: Please refer to Appendix B. ■

According to Proposition 1, when $\alpha=4$, the ASE of communication is generally a decreasing function of the cooperative cluster size L. This can be explained by the fact that the communication performance improvement brought by interference nulling cannot compensate for the performance loss caused by the reduction of the diversity/multiplexing gain for the average throughput of the networks. Thus, it is optimal retain all spatial dimensions for multiplexing and diversity. When $\alpha\to 2$, the conclusion in Proposition 1 can also be proved in a similar way.

B. Sensing Performance

First, under a given distance R from the serving BS to the typical target, we can derive the conditional radar information rate expectation as follows:

$$R_s=\int_0^{\infty}\frac{1-\mathrm{E}\left[e^{-z\xi\Delta T\kappa M_{\mathrm{r}}h_{j,1}^{t}}\right]}{z}\mathrm{E}\left[e^{-zI_{\mathrm{S}}}\right]dz, \tag{9}$$

where $I_{\mathrm{S}}=\sum_{q=Q+1}^{\infty}h_{q,1}\|\mathbf{d}_q-\mathbf{d}_1\|^{-\alpha}R^{2\beta}$. According to the analysis of the distribution of effective signals and interference signals, we have $\mathrm{E}\left[e^{-z\xi\Delta T\kappa M_{\mathrm{r}}h_{j,1}^{t}}\right]=(1+\xi\Delta T\kappa M_{\mathrm{r}}z)^{-K}$. We note that it is challenging to derive the radar information rate expression due to the special probability density function (PDF) of distance from the interfering BSs to the serving BS. Specifically, considering that the typical target is sensed by the closest BS, i.e., the serving BS, it is impossible to find another BS in the circle defined with the target as its center and a radius equal to the distance to the serving BS (namely interference hole).

To tackle the above issue, we analyze the exact PDF of interfering BS's distance from a perspective of geometry, and obtain a extremely tight expressions with $Q=1$ as follow.

Proposition 2: When $Q=1$, the average radar information rate R_s can be given by

$$R_s=\int_0^{\infty}\frac{1-(1+\xi\Delta T\kappa M_{\mathrm{r}}z)^{-K}}{z}\int_0^{\infty}\mathcal{L}_{I_{\mathrm{S}}}(z)f(R)dRdz, \tag{10}$$

where $f(R)=2\pi\lambda_b Re^{-\pi\lambda_b R^2}$ and $\mathcal{L}_{I_{\mathrm{S}}}(z)=\exp\Bigg(-R\Bigg(Kz^{\frac{2}{\beta}}\left(\frac{R}{\pi\lambda_b}\right)^{\frac{2\alpha}{\beta}-1}B\left(1,1-\frac{2}{\beta},K+\frac{2}{\beta}\right)+1-\int_0^2\frac{2}{\pi}\arccos\frac{t}{2}\left(1-\left(1+z\left(\frac{R}{\pi\lambda_b}\right)^{\alpha-\beta/2}t^{-\beta}\right)^{-K}\right)tdt\Bigg)\Bigg)$.

Proof: The effective transmit beamforming gain at the target's direction and sensing interference channel gain between BSs can be approximated as gamma random variables, i.e., $h_{j,1}^{t}$ and $h_{i,1}\sim\Gamma(K,1)$. The strip's area, formed by the intersection of the annular area with no interference and the serving BS's circle, can be represented as $2x\,\mathrm{d}x(\pi-\varphi(x))$, with $\varphi(x)=\arccos\left(\frac{x}{2R}\right)$ denoting the angle within the hole. Consequently, the Poisson distribution models the number of interfering points within this strip, with a mean of $\lambda_b 2x\,\mathrm{d}x(\pi-\varphi(x))$. Using this intermediate result, we now derive tight bounds on the Laplace transform of sensing interference as follows:

$$\begin{aligned}\mathcal{L}_{I_{\mathrm{S}}}(z)=&\exp\Bigg(-\pi\lambda_b Kz^{\frac{2}{\beta}}R^{\frac{4\alpha}{\beta}}B\left(1,1-\frac{2}{\beta},K+\frac{2}{\beta}\right)\\&+\lambda_b R^2\int_0^2 2\arccos\frac{t}{2}\left(1-\frac{1}{\left(1+zR^{2\alpha-\beta}t^{-\beta}\right)^{K}}\right)tdt\Bigg).\end{aligned} \tag{11}$$

In (11), the second part is to subtract the interference in the hole with the service BS as the center. By calculating the probability integral of the target distance R, we have

$$\begin{aligned}&\mathcal{L}_{I_{\mathrm{S}}}(z)=\\&\int_0^{\infty}\exp\Bigg(-R\Bigg(Kz^{\frac{2}{\beta}}\left(\frac{R}{\pi\lambda_b}\right)^{\frac{2\alpha}{\beta}-1}B\left(1,1-\frac{2}{\beta},K+\frac{2}{\beta}\right)+1\\&-\int_0^2\frac{2}{\pi}\arccos\frac{t}{2}\left(1-\left(1+z\left(\frac{R}{\pi\lambda_b}\right)^{\alpha-\beta/2}t^{-\beta}\right)^{-K}\right)tdt\Bigg)\Bigg)dR.\end{aligned} \tag{12}$$

Then, by plugging (12) into (9), the radar information rate can be expressed as

$$R_s=\int_0^{\infty}\frac{1-(1+\xi\Delta T\kappa M_{\mathrm{r}}z)^{-K}}{z}\int_0^{\infty}\mathcal{L}_{I_{\mathrm{S}}}(z)f(R)dRdz. \tag{13}$$

This completes the proof. ■

The density of BSs typically impacts the average sensing performance because of the varying path loss coefficients between effective signals and interference. However, when $Q \geq 2$, deriving a tractable expression for radar information rate becomes challenging due to the intricate PDF of interfering BSs. To address this challenge, we adopt an approximation method to obtain a tractable expression as follows.

Theorem 2: When $Q \geq 2$, the sensing ASE can be given by

$$T_s^{\mathrm{ASE}} = \int_0^\infty \frac{1-(1+\xi\Delta T\kappa M_{\mathrm{r}} z)^{-K}}{z}\tilde{I}_{\mathrm{S}}dz, \tag{14}$$

where $\tilde{I}_{\mathrm{S}} = \int_0^\infty \int_0^\infty \exp\left(-\pi\lambda_b\left(r_Q^2\left(\left(1+zR^{2\alpha}r_Q^{-\beta}\right)^{-K}-1\right)\right.\right.$
$\left.\left.+Kz^{\frac{2}{\beta}}R^{\frac{4\alpha}{\beta}}B\left(\frac{zR^{2\alpha}r_Q^{-\beta}}{zR^{2\alpha}r_Q^{-\beta}+1}, 1-\frac{2}{\beta}, K+\frac{2}{\beta}\right)\right)\right) f_{r_q}(r) f_R(r) \mathrm{d}R\mathrm{d}r_q$.

Proof: Please refer to Appendix C. ■

IV. System Optimization

In this section, we study the optimization of the cooperative ISAC networks to achieve a flexible balance between S&C. First, the weighted sum ASE is defined as a function of the S&C rates and given by

$$T^{\mathrm{ASE}} = \rho T_c^{\mathrm{ASE}} + (1-\rho)\, T_s^{\mathrm{ASE}}. \tag{15}$$

In (15), ρ represents the weighting factor of S&C performance. The problem formulation can be expressed as

$$(\mathrm{P1}): \max_{J,K,Q,L} \quad T^{\mathrm{ASE}} \tag{16}$$
$$\text{s.t.} \quad KL + J(Q-1) + 1 \leq M_{\mathrm{t}}, \tag{16a}$$
$$J, K, Q, L \geq 1, J \leq J_{\max}. \tag{16b}$$

A direct way to find the optimal value is to exhaustively search all feasible variables (K, L, J, Q). However, such an operation is with high computational complexity, especially when the number of transmit antennas is large.

It is observed that in (8), to maximize the communication ASE T_c^{ASE} efficiently, we can relax K to continuous variables and substituting $v = \frac{K}{M_{\mathrm{t}}-J(Q-1)+1}$ into (8), we have

$$T_c^{\mathrm{ASE}} = \lambda_b(M_{\mathrm{t}} - J(Q-1)+1)G(v), \tag{17}$$

where $G(v) = \int_0^\infty \frac{1-e^{-z\frac{\Gamma\left(L+\frac{\alpha}{2}\right)\left(\frac{1}{v}-L\right)}{\Gamma(L+1)\Gamma\left(1+\frac{\alpha}{2}\right)}}}{z\mathrm{F}(z,\alpha)}dz$. Therefore, we know that the optimal v^* is only related to variable L. The following lemma gives the optimal v^* to maximize T_c^{ASE}.

Proposition 3: With any given J and Q, the optimal K can be uniquely found by solving the following equation:

$$\int_0^\infty \frac{1-e^{-z\left(\frac{1}{v}-L\right)} - ze^{-z\left(\frac{1}{v}-L\right)}/v}{z\mathrm{F}(z,\alpha)}dz = 0. \tag{18}$$

Proof: $G(v)$ is a concave function with respect to v since the second-order derivative of $G(v)$ satisfies $G''(v) > 0$. The fist-order derivative of $G(v)$ is $G'(v) = \int_0^\infty \frac{1-e^{-z\left(\frac{1}{v}-L\right)} - ze^{-z\left(\frac{1}{v}-L\right)}/v}{z\mathrm{F}(z,\alpha)}dz$. Then, we have $\lim_{v\to 0} G'(v) = \int_0^\infty \frac{1}{z\mathrm{F}(z,\alpha)}dz > 0$, and $G'(1) = \int_0^\infty \frac{1-e^{-z(1-L)}-ze^{-z(1-L)}}{z\mathrm{F}(z,\alpha)}dz < 0$. Considering that $G(v)$ is a concave function and $G'(v) < 0$, there is always a unique solution v^* within $[0,1]$ to solve the equation $G'(v) = 0$. ■

Based on Proposition 3, the optimal K can be obtained by a binary search instead of a one-dimensional search. Moreover, with $L = 1$, the optimal ratio of scheduled users $\frac{K}{M_{\mathrm{t}}+1}$ is constant, which is also verified in simulations (c.f. Fig. 2). According to the Theorem 1, it can be verified that the communication ASE T_c^{ASE} decreases monotonically with the increase of $J(Q-1)$. The optimal communication part is to satisfy $\frac{K}{M_{\mathrm{t}}-J(Q-1)+1} = v$, where v can be deemed as a constant parameter with a given L. Therefore, (P1) can be solved more efficiently.

Furthermore, Let us consider the case that there are minimum service quality constraints for the users/targets being served/detected, i.e., $L \geq L^{th}$ and $Q \geq Q^{th}$. In this case, there is a new tradeoff between the average performance of S&C (R_s and R_c) and the whole network performance (T_s^{ASE} and T_c^{ASE}). To illustrate such a tradeoff, we formulate problem (P2) as follows:

$$(\mathrm{P2}): \max_{J,K,Q,L} \quad T_c^{\mathrm{ASE}} \tag{19}$$
$$\text{s.t.} \quad R_s \geq R_s^{th}, R_c \geq R_c^{th}, T_s^{\mathrm{ASE}} \geq T_c^{\mathrm{th}}, \tag{19a}$$
$$KL + J(Q-1) + 1 \leq M_{\mathrm{t}}, \tag{19b}$$
$$J, K, Q, L \geq 1, J \leq J_{\max}. \tag{19c}$$

By adopting similar conclusions in problem (P1), (P2) can also be solved efficiently, and the results are shown in Fig. 5.

V. Simulations

Numerical simulations are averaged over network typologies and small-scale channel fading realizations. The system parameters are given as follows: the number of transmit antennas $M_{\mathrm{t}} = 20$, the number of receive antennas $M_{\mathrm{r}} = 10$, the RCS $\xi = 0.1$, $\kappa = 1$, matching filter gain $\Delta T = 1$, the BS density $\lambda_b = 1/km^2$, $J_{\max} = 10$, pathloss coefficients $\alpha = 4$, and $\beta = 2$.

In Fig. 2, the tractable expressions obtained using Theorem 1 exhibit a notably close approximation to truth for $M_{\mathrm{t}} = 5$, $M_{\mathrm{t}} = 10$, and $M_{\mathrm{t}} = 20$, respectively. When optimizing the communication ASE, we observe that the ratio between the number of users and the number of BS antennas remains consistent at approximately 60% across various numbers of transmit antennas. This finding aligns with the analysis presented in Proposition 3. Furthermore, with fewer scheduled users, the increase in the number of transmit antennas leads to limited improvement in ASE performance. This is anticipated as optimal spatial resource allocation for multiplexing and diversity gain plays a crucial role in maximizing performance gains in ISAC networks. To validate the analysis regarding optimal spatial resource allocation for maximizing communication ASE T_c^{ASE}, we conducted a comparison of T_c^{ASE} across various values of L and K, as illustrated in Fig. 3. The analysis reveals that at the maximum communication ASE,

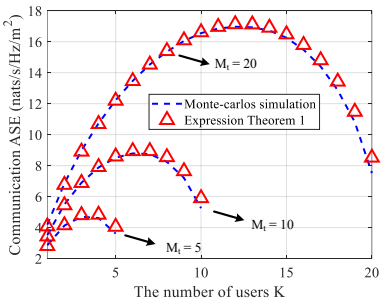

Fig. 2. Communication ASE with respect to K, with $L = 1$.

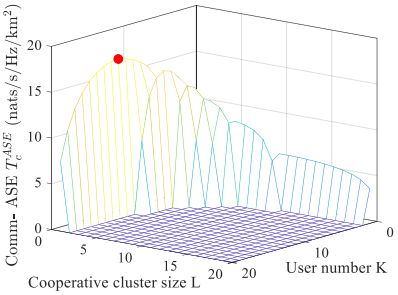

Fig. 3. Optimal cooperative cluster size L of the maximized communication ASE.

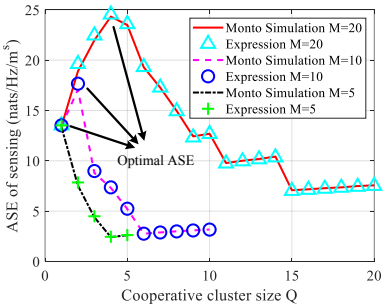

Fig. 4. Sensing ASE T_s^{ASE} comparisons with respect to cooperative sensing cluster size Q.

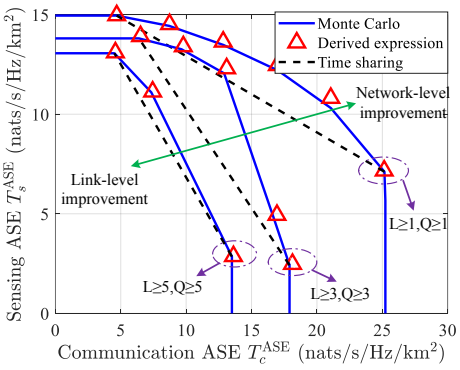

Fig. 5. ASE tradeoff between S&C versus different link-level constraints.

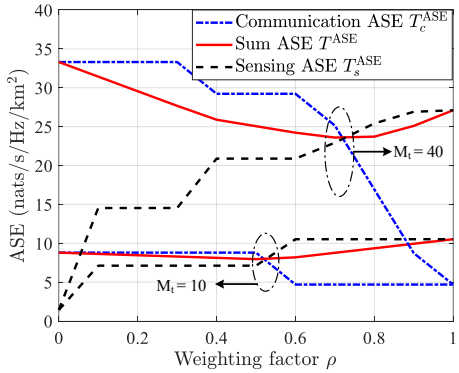

Fig. 6. Weighted sum ASE comparison with respect to weighting factor ρ.

the optimal values of K and L are 12 and 1 respectively. This indicates that there is no necessity for interference nulling to maximize communication ASE, affirming the conclusions drawn in Proposition 1.

As illustrated in Fig. 4, with $K = 1$ and $L = 1$, the accuracy of the derived expression for the sensing ASE is confirmed. We observe that the sensing ASE initially increases and then decreases as Q increases. Therefore, to maximize the sensing ASE, while the number of simultaneously sensed targets J may inevitably decrease, interference nulling for sensing with an appropriate cooperative cluster size can effectively enhance the sensing ASE. This expectation arises because interference does not suffer from round-trip path loss like echo signals, and it is possible that the distance from other interfering BSs to the sensor may be shorter than that from the target. Specifically, with $M_{\mathrm{r}} = 20$, our proposed cooperative scheme can attain up to twice the ASE compared to the scenario without interference nulling. Furthermore, as $J(Q-1)$ must be an integer, increasing the cooperative cluster size may necessitate appropriately reducing J to fulfil the DoF constraints (c.f. (16a)). This fluctuation in J results in variations of the sensing ASE as the cooperative cluster size increases.

In Fig. 5, with $M_{\mathrm{t}} = 30$, the boundary comparison of network performance under various link-level quality constraints is depicted, denoted by $L \geq L^{th}$ and $Q \geq Q^{th}$. Here, Q^{th} and L^{th} represent the minimum cooperative cluster sizes needed to attain the required S&C quality for the served targets or users. The relationship between the link quality constraint and network performance boundary is evident: as the link quality constraint becomes stricter, the network performance boundary decreases. This effect primarily stems from the constraint that limits the optimization range of variables L and Q, thereby reducing the DoF available for balancing the network performance of S&C. Figure 6 illustrates the optimal weighted summation ASE T^{ASE} for problem (P1) across varying weighting factors ρ. As the weighting coefficient ρ increases, the sensing ASE monotonically increases while the communication ASE decreases. Furthermore, it is observed that T^{ASE} is consistently lower than the maximum of the sensing ASE and the communication ASE. This is because the weighted summation ASE value always lies between the sensing-only ASE and the communication-only ASE.

VI. Conclusion

In this paper, we introduced a novel cooperative scheme for ISAC networks by leveraging coordinated beamforming. We demonstrated that interference nulling is unnecessary when maximizing communication ASE, whereas it is essential when maximizing sensing ASE. We formulated two optimization problems to assess ISAC network performance, confirming that optimal spatial resource allocation effectively enhances cooperative gain. Our simulation results offer valuable insights for the design of practical ISAC networks.

APPENDIX A: PROOF OF THEOREM 1

Specifically, according to equation (5) in [14], the coverage probability can be approximated by $P_L(\gamma) = P_1(\gamma/G_L)$, where γ is the SIR threshold and G_L denotes the effective gain by adopting interference nulling in the cooperative cluster. Then, under the given distance from the typical user to the serving BS r, the conditional expectation can be further approximated as follows:

$$\begin{aligned} R_c \approx & \mathrm{E}_{\Phi_b}\left[\log\left(1+\frac{\mathrm{E}\left[g_{k,1}^k\right]}{\sum_{i=L+1}^{\infty}\mathrm{E}\left[g_{k,i}\right]\|\mathbf{d}_i\|^{-\alpha}r^{\alpha}}\right)\right] \\ = & \int_0^{\infty}\frac{1-e^{-z\frac{M_{\mathrm{t}}-KL-J(Q-1)+1}{K}}}{z}\mathrm{E}\left[e^{-zI_{\mathrm{C}}}\right]dz. \end{aligned} \tag{20}$$

Then, the Laplace transform of communication interference with $L=1$ can be given by

$$\begin{aligned} \mathrm{E}\left[e^{-zI_{\mathrm{C}}}\right] = & \exp\Bigg(-\pi\lambda x\left(1-e^{-zr^{\alpha}x^{-\alpha/2}}\right)\Big|_{r^2}^{\infty} \\ & -\pi\lambda\int_{r^2}^{\infty}\frac{\alpha}{2}zr^{\alpha}x^{-\frac{\alpha}{2}}e^{-zr^{\alpha}x^{-\alpha/2}}dx\Bigg) \\ = & \exp\left(-\pi\lambda r^2\left(\mathrm{F}\left(z,\alpha\right)-1\right)\right), \end{aligned} \tag{21}$$

where $\mathrm{F}\left(z,\alpha\right) = e^{-z}+z^{\frac{2}{\alpha}}\Gamma\left(1-\frac{2}{\alpha},z\right)$. By plugging $\mathrm{E}\left[e^{-zI_{\mathrm{C}}}\right]$ and (20) into $\int_0^{\infty}\mathrm{E}_{g,\Phi_b}\left[\log\left(1+\mathrm{SIR}_c\right)\middle|r\right]f_r\left(r\right)dr$, we have $\mathrm{E}_{g,\Phi_b}\left[\log\left(1+\mathrm{SIR}_c\right)\right] = \int_0^{\infty}\exp\left(-\pi\lambda r^2(\mathrm{F}\left(z,\alpha\right)-1)\right)f(r)dr = \frac{1}{\mathrm{F}(z,\alpha)}$. Then, we need to further obtain the effective gain of SIR with L cooperative BSs compared to the case with $L=1$. According to [14], we can obtain an approximate coverage probability with $L-1$ interference nulling based on no-interference nulling case, i.e., $P_L(\gamma) = P_1(\gamma/G_L)$, where $G_L = \frac{\Gamma\left(L+\frac{\alpha}{2}\right)}{\Gamma(L+1)\Gamma\left(1+\frac{\alpha}{2}\right)}$ and $P_L(\gamma)$ denotes the coverage probability with SIR threshold γ. Therefore, $\frac{\mathrm{E}\left[g_{k,1}^k\right]}{\sum_{i=L+1}^{\infty}\mathrm{E}[g_{k,i}]\|\mathbf{d}_i\|^{-\alpha}r^{\alpha}}$ and $\frac{\mathrm{E}\left[g_{k,1}^k\right]G_L}{\sum_{i=2}^{\infty}\mathrm{E}[g_{k,i}]\|\mathbf{d}_i\|^{-\alpha}r^{\alpha}}$ follow nearly identical distributions. Then, it follows that

$$R_c \approx \int_0^{\infty}\frac{1-e^{-z\frac{\Gamma\left(L+\frac{\alpha}{2}\right)(M_{\mathrm{t}}-J(Q-1)+1-KL)}{K\Gamma(L+1)\Gamma\left(1+\frac{\alpha}{2}\right)}}}{z\mathrm{F}(z,\alpha)}dz. \tag{22}$$

Plugging (22) into 6, this thus completes the proof.

APPENDIX B: PROOF OF PROPOSITION 1

When $\alpha = 4$, $G_L = \frac{L+1}{2}$. For any given K, Q, J, we have $\frac{\Gamma\left(L+\frac{\alpha}{2}\right)}{\Gamma(L+1)\Gamma\left(1+\frac{\alpha}{2}\right)}\frac{M_{\mathrm{t}}-KL-J(Q-1)+1}{K} = \frac{1}{2}\left(-L^2+\left(\frac{M_{\mathrm{t}}-J(Q-1)+1}{K}-1\right)L+\frac{M_{\mathrm{t}}-J(Q-1)+1}{K}\right) \triangleq y(L)$. $y(L)$ is a quadratic function about L. It can be found that when $\frac{M_{\mathrm{t}}-J(Q-1)-K+1}{2K} \leq 1$, $y(L)$ is maximized when $L=1$. Otherwise, $y(L)$ is maximized when $L = \frac{M_{\mathrm{t}}-J(Q-1)-K+1}{2K}$, let $v = \frac{K}{M_{\mathrm{t}}-J(Q-1)+1}$, we have

$$\frac{\partial T_c^{\mathrm{ASE}}}{\partial v} = \int_0^{\infty}\frac{1-\left(1+z\frac{1+v}{2v^2}\right)e^{-z\frac{1}{4}\left(\frac{1}{v}+1\right)^2}}{zF(z,\alpha)}dz \geq 0. \tag{23}$$

Thus, in this case with $\frac{M_{\mathrm{t}}-J(Q-1)-K+1}{2K} \geq 1$, T_c^{ASE} is a monotonically increasing function with respect to K. Since $K \leq \frac{M_{\mathrm{t}}-J(Q-1)+1}{3}$, $y(L)$ is maximized with $K = \frac{M_{\mathrm{t}}-J(Q-1)+1}{3}$, and in this case, $L = \frac{M_{\mathrm{t}}-J(Q-1)+1}{2K}-\frac{1}{2} = 1$. Combining the above analysis, we complete the proof.

APPENDIX C: PROOF OF THEOREM 2

It can be readily found that the interference term in the hole can be ignored when $Q \gg 1$. Thus, to simplify the expression derivation, we remove the second term in (10) for the case with $Q \geq 2$, and then the conditional Laplace transform of sensing interference can be given by

$$\begin{aligned} \left[e^{-zI_{\mathrm{S}}}\middle|R,r_Q\right] = & \exp\Bigg(-\pi\lambda_b\Bigg(r_Q^2\left(\left(1+zR^{2\alpha}r_Q^{-\beta}\right)^{-K}-1\right) \\ & +Kz^{\frac{2}{\beta}}R^{\frac{4\alpha}{\beta}}B\left(\frac{zR^{2\alpha}r_Q^{-\beta}}{zR^{2\alpha}r_Q^{-\beta}+1},1-\frac{2}{\beta},K+\frac{2}{\beta}\right)\Bigg)\Bigg). \end{aligned} \tag{24}$$

Then, the Laplace transform of sensing interference is $\left[e^{-zI_{\mathrm{S}}}\right] = \int_0^{\infty}\int_0^{\infty}\left[e^{-zI_{\mathrm{S}}}\middle|R,r_q\right]f_{r_q}\left(r\right)f_R(r)dRdr_q$. Finally, by plugging $\left[e^{-zI_{\mathrm{S}}}\right]$ into (9) and (6), the tractable expressions of the radar information rate and sensing ASE can be obtained.

REFERENCES

[1] J. A. Zhang *et al.*, "An overview of signal processing techniques for joint communication and radar sensing," *IEEE J. Sel. Top. Signal Process.*, vol. 15, no. 6, pp. 1295–1315, 2021.

[2] K. Meng, Q. Wu, W. Chen, and D. Li, "Sensing-assisted communication in vehicular networks with intelligent surface," *IEEE Trans. Veh. Technol.*, pp. 1–17, 2023.

[3] Y. Cui, F. Liu, X. Jing, and J. Mu, "Integrating sensing and communications for ubiquitous IoT: Applications, trends, and challenges," *IEEE Net.*, vol. 35, no. 5, pp. 158–167, Sep./Oct. 2021.

[4] K. Meng *et al.*, "Throughput maximization for UAV-enabled integrated periodic sensing and communication," *IEEE Trans. Wireless Commun.*, vol. 22, no. 1, pp. 671–687, Jan. 2023.

[5] W. Shin *et al.*, "Coordinated beamforming for multi-cell MIMO-NOMA," *IEEE Commun. Lett.*, vol. 21, no. 1, pp. 84–87, Jan. 2017.

[6] J. G. Andrews, F. Baccelli, and R. K. Ganti, "A tractable approach to coverage and rate in cellular networks," *IEEE Trans. Commun.*, vol. 59, no. 11, pp. 3122–3134, Nov. 2011.

[7] M. Di Renzo and P. Guan, "Stochastic geometry modeling and system-level analysis of uplink heterogeneous cellular networks with multi-antenna base stations," *IEEE Trans. Commun.*, vol. 64, no. 6, pp. 2453–2476, Jun. 2016.

[8] W. Chen, L. Li, Z. Chen, B. Ning, G. Wang, and T. Quek, "An ISAC-based beam alignment approach for enhancing terahertz network coverage," *arXiv preprint arXiv:2212.01728*, 2022.

[9] A. Salem, K. Meng, C. Masouros, F. Liu, and D. López-Pérez, "Rethinking dense cells for integrated sensing and communications: A stochastic geometric view," *arXiv preprint arXiv:2212.12942*, 2022.

[10] J. Park, N. Lee, J. G. Andrews, and R. W. Heath, "On the optimal feedback rate in interference-limited multi-antenna cellular systems," *IEEE Trans. Wireless Commun.*, vol. 15, no. 8, pp. 5748–5762, Aug. 2016.

[11] M. Ding, D. Lopez-Perez, G. Mao, P. Wang, and Z. Lin, "Will the area spectral efficiency monotonically grow as small cells go dense?" in *IEEE Proc. GLOBECOM*, 2015, pp. 1–7.

[12] Y. Yang and R. S. Blum, "MIMO radar waveform design based on mutual information and minimum mean-square error estimation," *IEEE Trans. Aerosp. Electron. Syst.*, vol. 43, no. 1, pp. 330–343, Jan. 2007.

[13] K. A. Hamdi, "A useful lemma for capacity analysis of fading interference channels," *IEEE Trans. Commun.*, vol. 58, no. 2, pp. 411–416, Feb. 2010.

[14] M. Haenggi, "The mean interference-to-signal ratio and its key role in cellular and amorphous networks," *IEEE Wireless Commun. Lett.*, vol. 3, no. 6, pp. 597–600, Dec. 2014.